Modeling and Optimization of a Novel Membrane Reformer for Higher Hydrocarbons

Zhongxiang Chen, Yibin Yan, and Said S. E. H. Elnashaie
Chemical Engineering Dept., Auburn University, Auburn, AL 36849

A novel circulating fast fluidized-bed membrane reformer efficiently carries out simultaneous steam and oxidative reforming of heptane over nickel catalysts. A plug-flow reactor model was developed to investigate effects of the operating parameters. The cases with palladium hydrogen membranes and/or dense perovskite oxygen membranes are investigated. The simulations show that high purity hydrogen can be efficiently produced using hydrogen membranes, which "break" the thermodynamic equilibrium barriers. The perovskite oxygen selective membranes supply oxygen along the length (or height) of the reformer for oxidative reforming of hydrocarbons, providing the heat necessary for the highly endothermic steam reforming reaction. The combination of these two membranes with the characteristics of the fast fluidization reformer makes this process not only an efficient hydrogen producer but also an energy efficient process. The fast continuous flow of catalyst makes the effect of carbon deposition on catalyst activity negligible in the novel process. Process optimization for the maximum hydrogen yield is conducted using the flexible tolerance optimization method.

Introduction

Currently, steam reforming of hydrocarbons is the main process for hydrogen production (Rostrup-Nielsen, 1973, 1977; Tottrup, 1982; Christensen, 1996; Xu and Froment, 1989; Elnashaie and Elshishini, 1993; Ding and Alpay, 2000; Froment, 2000; Hou et al., 2000). Natural gas (mainly methane) has become the most important and economical feedstock because of its abundant availability (Twigg, 1989; Armor, 1999). However, steam reforming of higher hydrocarbons can be quite attractive for the chemical and petrochemical industries (Phillips et al., 1969; Rostrup-Nielsen, 1973, 1977; Tottrup, 1982; Christensen, 1996), especially at some places where natural gas is not abundant such as Japan and the United States (Rostrup-Nielsen, 1977; Twigg, 1989). Rostrup-Nielsen (1977), Tottrup (1982), and Christensen (1996) used heptane as the model feed for the investigations of steam reforming of higher hydrocarbons. Avc and his coworkers (2001) have assumed that the kinetics of steam reforming of octane is the same as that of heptane in their hydrogen fuel cell studies, where octane is used as a model feed for gasoline.

Correspondence concerning this article should be addressed to Z. Chen.

Most commercial reforming catalysts are nickel-based because of its high efficiency and relatively low cost. However, the catalyst suffers from deactivation due to carbon formation. To avoid carbon formation, high steam-to-carbon feed ratio in the range of 2–5 is commonly utilized in industrial fixed-bed reformers (Elnashaie and Elshishini, 1993). In order to avoid excessive pressure drop in industrial fixed-bed reformers, large catalyst particles are used, resulting in an extremely low effectiveness factor η ($\sim 10^{-2}$–10^{-3}) (Rostrup-Nielsen, 1977; Elnashaie et al., 1988; Alhabdan et al., 1992). This severe diffusional limitation "problem" can be "solved" by using fine catalyst particles in fluidized-bed reactors ($\eta \cong 1.0$). Earlier trials to improve this process through the use of fine catalyst involved the use of bubbling fluidized beds (Elnashaie and Adris, 1989; Adris et al., 1991, 1994a, 1997; Roy et al., 1999) and proved to be very successful. The bubbling fluidized-bed process has reached the stage of a successful pilot plant testing (Adris et al., 1994a, 1994b, 1997; Roy et al., 1999). However, the bubbling fluidized-bed reformer is not the final answer to the efficient production of hydrogen through steam reforming. It still suffers from some important limitations such as the fluid dynamic limitation and the lack of the possibility for continuous catalyst regenera-

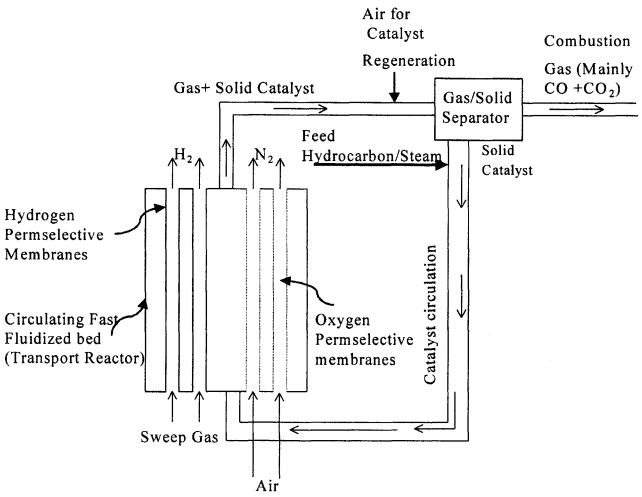

Figure 1. Novel process consisting of a circulating fast fluidized-bed membrane reformer (CFFBMR).

tion, and, therefore, it is not suitable for steam reforming of higher hydrocarbons (diesel, bio-oil, and so on) because of the excessive carbon formation associated with those feedstocks in a system with stationary catalyst.

To improve this process further, a novel more efficient and flexible process has been proposed (Chen et al., 2002). As shown in Figure 1, it consists of a circulating fast fluidized-bed membrane reformer (CFFBMR), which is similar, in principle, to modern FCC units. Inside this novel reformer, there are a number of palladium-based hydrogen permselective membrane tubes and/or dense perovskite oxygen permselective membrane tubes. Between these membrane tubes, the nickel reforming catalyst is fast fluidized, and steam reforming of higher hydrocarbons takes place. The product hydrogen permeates selectively through hydrogen membranes from the reaction side and is carried away by sweep gas such as low-value steam in the hydrogen membrane tubes. Air is fed into the oxygen-selective membrane tubes, where oxygen permeates into the reaction side for oxidative reforming (or partial oxidation) of hydrocarbons. The deactivated catalyst is carried out of the reformer with the exit gas stream, regenerated along the exit line of the CFFBMR and separated in a gas–solid separator. The regenerated catalyst is recycled to the riser reformer. The fast flow of catalyst makes the effect of carbon deposition on the catalyst activity negligible; besides, in the full process the carbon is completely burned and the catalyst is fully regenerated.

In this introductory investigation, mathematical simulation and optimization are carried out only on the reactor section of the CFFBMR. The cases without/with hydrogen and/or oxygen permselective membranes in the novel CFFBMR are investigated. Heptane is used as a model higher hydrocarbon.

Reaction Kinetics

Kinetics of steam reforming of heptane and methane

Many researchers have used the following reactions to study steam reforming of higher hydrocarbons on nickel catalysts (Phillips et al., 1969; Rostrup-Nielsen, 1973, 1977; Tottrup, 1982; Christensen, 1996). The steam-reforming reaction (Eq. 1) is considered to be irreversible for all higher hydrocarbons, and higher hydrocarbons are converted into C_1-components (methane and carbon oxides) with no intermediates (Christensen, 1996). Methane and carbon dioxide are produced by methanation (Eq. 2) and (Eq. 3) water gas shift reactions

$$C_nH_m + nH_2O \rightarrow nCO + \left(n + \frac{1}{2}m\right)H_2 \quad (1)$$

$$CO + 3H_2 \rightleftharpoons CH_4 + H_2O \quad \Delta H^o_{298} = -206.2\ \text{kJ/mol} \quad (2)$$

$$CO + H_2O \rightleftharpoons CO_2 + H_2 \quad \Delta H^o_{298} = -41.2\ \text{kJ/mol} \quad (3)$$

In this article heptane is used as a model higher hydrocarbon, and, therefore, the reaction (Eq. 1) can be written as

$$C_7H_{16} + 7H_2O \rightarrow 7CO + 15H_2 \quad \Delta H^o_{298} = 1108\ \text{kJ/mol} \quad (1')$$

Tottrup (1982) provided an intrinsic kinetic equation (Eq. 4) for the irreversible reaction (Eq. 1′)

$$r_1 = \frac{8\times 10^5 e^{-67{,}800/RT} P_{C_7H_{16}}}{\left[1 + 25.2\dfrac{P_{C_7H_{16}}P_{H_2}}{P_{H_2O}} + 0.077\dfrac{P_{H_2O}}{P_{H_2}}\right]^2}\ \text{mol/gcat}\cdot h \quad (4)$$

where r_1 is the generalized reaction rate for steam reforming of heptane; $P_{C_7H_{16}}$, P_{H_2}, P_{H_2O} are partial pressures of heptane, hydrogen, and steam, respectively; R is the gas constant, 8.314 J/mol/K; T is the reaction temperature.

The reforming gas is rich in methane due to the methanation reaction (Eq. 2), and therefore steam reforming of methane takes place. The most general reactions and kinetics for methane steam reforming can be obtained from Xu and Froment (1989)

$$CH_4 + H_2O \rightleftharpoons CO + 3H_2$$

$$r_2 = k_1\left(\frac{P_{CH_4}P_{H_2O}}{P_{H_2}^{2.5}} - \frac{P_{CO}P_{H_2}^{0.5}}{K_1}\right)/DEN^2 \quad \text{mol/gcat}\cdot\text{h} \quad (5)$$

$$CO + H_2O \rightleftharpoons CO_2 + H_2$$

$$r_3 = k_2\left(\frac{P_{CO}P_{H_2O}}{P_{H_2}} - \frac{P_{CO_2}}{K_2}\right)/DEN^2 \quad \text{mol/gcat}\cdot\text{h} \quad (6)$$

$$CH_4 + 2H_2O \rightleftharpoons CO_2 + 4H_2$$

$$r_4 = k_3\left(\frac{P_{CH_4}P_{H_2O}^2}{P_{H_2}^{3.5}} - \frac{P_{CO_2}P_{H_2}^{0.5}}{K_2\cdot K_1}\right)/DEN^2 \quad \text{mol/gcat}\cdot\text{h} \quad (7)$$

where the term DEN is given by

$$DEN = 1 + K_{CO}P_{CO} + K_{H_2}P_{H_2} + K_{CH_4}P_{CH_4} + K_{H_2O}P_{H_2O}/P_{H_2} \quad (8)$$

and r_2, r_3, r_4 are the generalized reaction rates for steam reforming of methane and water gas shift reactions (Eqs. 5, 6,

and 7), respectively; P_{CH_4}, P_{CO}, P_{CO_2} are the partial pressures of methane, carbon monoxide, and carbon dioxide, respectively; K_1, K_2 are equilibrium constants for reaction (Eq. 5) and water gas shift reaction (Eq. 6); k_1, k_2, k_3 are rate constants for reactions (Eqs. 5, 6, and 7); K_{CH_4}, K_{CO}, K_{H_2}, K_{H_2O} are adsorption equilibrium constants of methane, carbon monoxide, hydrogen, and steam, respectively.

Kinetics of oxidative reforming of heptane and methane

The main advantage of oxidative reforming of hydrocarbons is the reaction exothermicity that supplies the heat needed for the endothermic steam reforming. In the CFFBMR oxygen can be supplied by direct feed or through oxygen membranes. Because methane is a rich product gas, oxidative reforming of methane takes place, too. Oxidative reforming of heptane can be represented by the following reaction where the products are CO and H_2 rather than CO_2 and H_2

$$C_7H_{16} + 3.5O_2 \rightarrow 7CO + 8H_2 \tag{9}$$

The kinetic rate for oxidative reforming of heptane can be obtained from Siminski et al. (1972)

$$r_5 = 75.9e^{-(101{,}431/RT)}TP^{0.3}C_{C_7H_{16}}^{0.5}C_{O_2} \quad \text{mol/gcat}\cdot\text{h} \tag{10}$$

where r_5 is the generalized reaction rate for oxidative reforming of heptane; P is the reaction pressure; $C_{C_nH_m}$, C_{O_2} are molar concentrations of hydrocarbon heptane and oxygen.

The general mechanism for oxidative reforming (or partial oxidation) of methane over nickel reforming catalyst proposed by Ashcroft and his coworkers (1990) is the combustion of methane followed by both steam and carbon dioxide reforming. Many researchers used this mechanism (Blank et al., 1990; Groote and Froment, 1996; Ostrowski et al., 1998; Wurzel et al., 1998, and Jin et al., 2000). Jin and his coworkers (2000) presented a group of kinetic equations for oxidative reforming of methane as follows

$$CH_4 + 2O_2 \rightarrow CO_2 + 2H_2O$$

$$r_6 = 3.96\times10^3 e^{-(166{,}000/RT)}P_{CH_4}P_{O_2} \quad \text{mol/gcat}\cdot\text{h} \tag{11}$$

$$CH_4 + H_2O \rightleftharpoons CO + 3H_2$$

$$r_7 = 1.51\times10^{-5}e^{-(29{,}000/RT)}P_{CH_4}P_{H_2O}\left(1 - \frac{P_{CO}P_{H_2}^3}{K_5P_{CH_4}P_{H_2O}}\right) \quad \text{mol/gcat}\cdot\text{h} \tag{12}$$

$$CH_4 + CO_2 \rightleftharpoons 2CO + 2H_2$$

$$r_8 = 8.71\times10^{-6}e^{-(23{,}700/RT)}P_{CH_4}P_{CO_2}\left(1 - \frac{P_{CO}^2P_{H_2}^2}{K_6P_{CH_4}P_{CO_2}}\right) \quad \text{mol/gcat}\cdot\text{h} \tag{13}$$

where r_6, r_7, r_8 are the generalized reaction rates for methane combustion, steam reforming, and carbon dioxide reforming of methane (Eqs. 11, 12 and 13), respectively; K_5, K_6 are the reaction equilibrium constants; and P_{O_2} is partial pressures of oxygen.

Because the methanation (Eq. 2) is the reverse of methane steam reforming (Eq. 5), the partial pressures of the different components in the gas mixture determine the direction of the reaction. The mechanism of oxidative reforming of methane also includes the step of steam reforming of methane (Eq. 12), which is the same as the reaction (Eq. 5). Therefore, only the kinetic rate of the reaction (Eq. 5) is used for the complete reaction kinetics in this article.

Characteristics of Fast Fluidized Bed

It is well known that in a fluidized bed if the gas velocity exceeds the solid particle free-fall terminal velocity, u_t, the particles will be carried upward and out of the reactor. This state is called fast fluidization. For fine particles, the Reynolds numbers, Re_P, will be small and the terminal velocity, u_t, can be obtained using Kunii and Levenspiel's equations (1991)

$$u_t = \frac{g(\rho_C - \rho_g)d_P^2}{18\mu} \qquad Re_P < 0.4 \tag{14}$$

$$u_t = \left\{\frac{1.78\times10^{-2}\left[g(\rho_C - \rho_g)\right]^2}{\rho_g\mu}\right\}^{1/3} d_P \quad 0.4 < Re_P < 500 \tag{15}$$

where g is gravitational acceleration, ρ_C, ρ_g are densities of solid particles and gas, respectively; d_p is the diameter of solid particles; and μ is gas viscosity, respectively.

Haider and Levenspiel (1989) have provided this terminal velocity for any shaped particles of sphericity ψ as follows

$$u_t = u_t^*\left[\frac{(\rho_C - \rho_g)g\mu}{\rho_g^2}\right]^{1/3} \tag{16}$$

where u_t^* and d_p^* are dimensionless terminal velocity and particle diameter, which are given by

$$u_t^* = \left[\frac{18}{(d_P^*)^2} + \frac{2.335 - 1.744\psi}{(d_P^*)^{0.5}}\right]^{-1} \tag{17}$$

$$d_P^* = d_P\left[\frac{\rho_g(\rho_C - \rho_g)g}{\mu^2}\right]^{1/3} \tag{18}$$

Grace (1986) has provided a graph to show the expected behavior of gas–solid fluidized system. Figure 2 shows a modification of this graph (Kunii and Levenspiel, 1997), by which the operating range of the gas velocity for fast fluidization can be determined.

Modeling of CFFBMR and Simulation Conditions

The fast fluidized-bed reformer is modeled as a plug-flow reactor with cocurrent flow in the reactor and membrane sides. The following assumptions are made for the modeling:

(1) Plug flow on both the reaction side and permeation membrane sides;

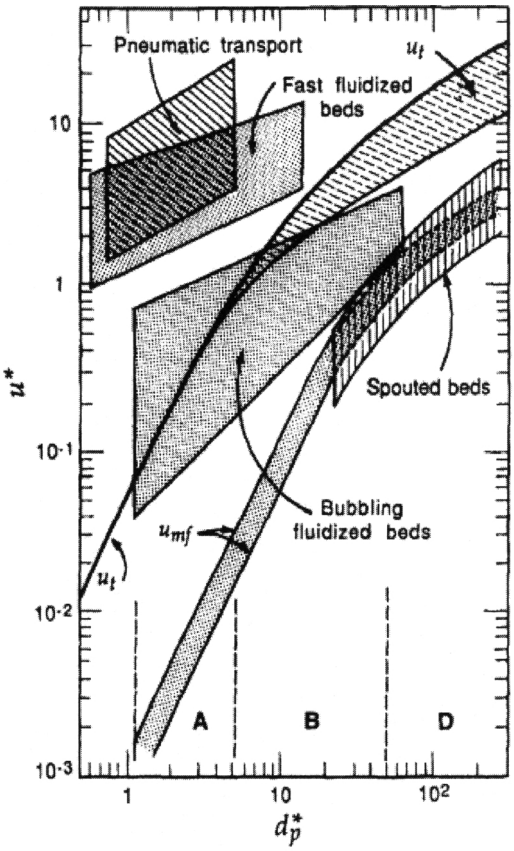

Figure 2. Generalized gas and solid fluidized systems.
From Grace, 1986; Kunii and Levenspiel, 1997.

(2) The operating pressures in the reactor, hydrogen, and/or oxygen membranes are constant;

(3) The palladium hydrogen (or dense perovskite oxygen) permselective membrane is 100% selective for hydrogen (or oxygen);

(4) Steady-state operations;

(5) Since fine powder catalysts (mean diameter is 186 μm) are used, there is no diffusional limitations in the reactor, that is, intrinsic reaction kinetics are used;

(6) The velocities of gas and solid are the same, there is no "slip" between the solid and gas phases;

(7) There is no hydrogen oxidation taking place over a nickel reforming catalyst;

(8) Ideal gas law is used to calculate the partial pressures in the reactor and membrane sides;

(9) The heat capacities of the components are constant;

(10) The temperature profiles in the reaction side and membrane tubes are the same;

(11) The sweep gas in the hydrogen membranes is inert;

(12) Due to the large mass flow ratio of catalyst to gas in the CFFBMR and the fully regeneration of catalyst along the exit line of the CFFBMR before recycling to the riser reformer, the effect of carbon deposition on the catalyst activity is negligible;

(13) The oxygen introduction into the membrane reformer will not oxidize the palladium-based hydrogen selective membranes.

The steady-state model equations for material and energy balances in the reaction side are given by

$$\frac{dF_i}{dl} = \rho_C(1-\epsilon)\cdot A_f \cdot \sum_{j=1}^{J} \sigma_{i,j} r_j - a\cdot J_{H_2}\cdot \pi \cdot N_{H_2}\cdot d_{H_2} + b\cdot J_{O_2}\cdot \pi \cdot N_{O_2}\cdot d_{O_2} \quad (19)$$

$$\frac{dT}{dl} = \frac{\sum_{j=1}^{J} r_j(-\Delta H_j)\,\rho_C(1-\epsilon)A_f + \dot{Q}}{\sum F_i Cp_i} \quad (20)$$

where F_i is the molar flow rate of component i; l is the reactor length; ρ_c is the density of catalyst; ϵ is the void fraction; A_f is the free cross-sectional area of the reactor; $\sigma_{i,j}$ is the stoichiometric coefficient of component i for the reaction j; r_j is the rate of the reaction j; J_{H_2}, J_{O_2} are permeation fluxes of hydrogen and oxygen; d_{H_2}, d_{O_2} are diameters of the hydrogen and oxygen membrane tubes; N_{H_2}, N_{O_2} are the number of hydrogen and oxygen membrane tubes, respectively; a and b are the control indexes for the membrane fluxes for the hydrogen and oxygen components, when for the component hydrogen, $a=1$ and $b=0$; for the component oxygen, $a=0$ and $b=1$; for the other components i, $a=0$ and $b=0$; ΔH_j is the heat of reaction for the reaction j; $\dot{Q}$ is the heating rate along the reactor length; and Cp_i is the specific heat of component i.

For material balance in hydrogen permeation membrane tubes

$$\frac{dF_{H_2,p}}{dl} = J_{H_2}\cdot \pi \cdot N_{H_2}\cdot d_{H_2} \quad (21)$$

where the subscript of p stands for the membrane permeation sides.

For material balance in oxygen permeation membrane tubes

$$\frac{dF_{O_2,p}}{dl} = -J_{O_2}\cdot \pi \cdot N_{O_2}\cdot d_{O_2} \quad (22)$$

In the CFFBMR the fluxes of hydrogen and oxygen are dependent on the type of membranes used. For a supported dense palladium (Pd) membrane, the hydrogen permeation flux will have the form (Shu et al., 1994; Barbieri and Maio, 1997)

$$J_{H_2} = -\frac{Q_{H_2}}{\delta_{H_2}}\exp\left(\frac{-E_{H_2}}{RT}\right)\left(\sqrt{p_{H_2,r}} - \sqrt{p_{H_2,p}}\right) \quad (23)$$

For a dense perovskite oxygen-permeable membrane, the oxygen permeation flux will have the form (Tsai et al., 1997)

$$J_{O_2} = Q_{O_2}\exp\left(\frac{-E_{O_2}}{RT}\right)\frac{T}{\delta_{O_2}}\ln\left(\frac{P_{O_2,p}}{P_{O_2,r}}\right) \quad (24)$$

where Q_{H_2}, Q_{O_2} are preexponential factors for the permeability of hydrogen and oxygen; δ_{H_2}, δ_{O_2} are the thickness of hydrogen and oxygen membranes; E_{H_2}, E_{O_2} are the activation energies for hydrogen and oxygen permeation; the subscript r stands for the reaction side.

Table 1. The Base Set of Simulation Conditions

Reformer tubes and membrane tubes		
Length of reformer tube and membrane tubes		2 m
Diameter of the reformer tube		0.0978 m
Number of reactor tubes		1
Diameter of hydrogen membrane tubes		0.00489 m
Thickness of hydrogen membrane tubes		20 μm
Diameter of oxygen permeable membrane tubes		0.00489 m
Thickness of oxygen permeable membrane tube		55 μm
Catalyst pellet		
Shape of particles		Fine sphere
Diameter (mean size)		186 μm
Particle density		2835 kg/m^3
Void fraction of reformer		0.8
Mass flow of catalyst		11.37 kg/s
Process gas feed rate and composition		
Component *i*	kmol/h	mol/s
C_7H_{16}	0.64	0.1778
H_2	0.01	0.002778
H_2O	9	2.5
Sweep gas in membranes		
	Flow rate (mol/s)	Pressure (atm)
Steam in hydrogen membrane	0.2778	1
Air in oxygen membrane	2.778	30
Reaction condition		
Reaction temperature		723 K (or 450°C)
Reaction pressure		10 atm
Steam-to-carbon ratio (S/C)		2 mol/mol
Catalyst-to-carbon (of heptane) mass flow ratio (g/g)		761.3

The method given by Kunii and Levenspiel (1997), as reviewed earlier, has been used to verify that the novel reformer is operating in the fast fluidization regime during the simulation and optimization investigation. The base set of simulation conditions are listed in Table 1, in which the main parameters of reformer and catalyst are chosen based on industrial fixed-bed reformers for steam reforming of methane (Elnashaie and Elshishini, 1993).

Simulation Results and Discussions

Isothermal operations: effect of temperature without/with hydrogen selective membranes

The effect of the reactor temperature is investigated at 623, 723 and 823 K under isothermal conditions without and with only 10 hydrogen membrane tubes (no oxygen membranes). Figure 3 shows that the conversion of heptane increases as

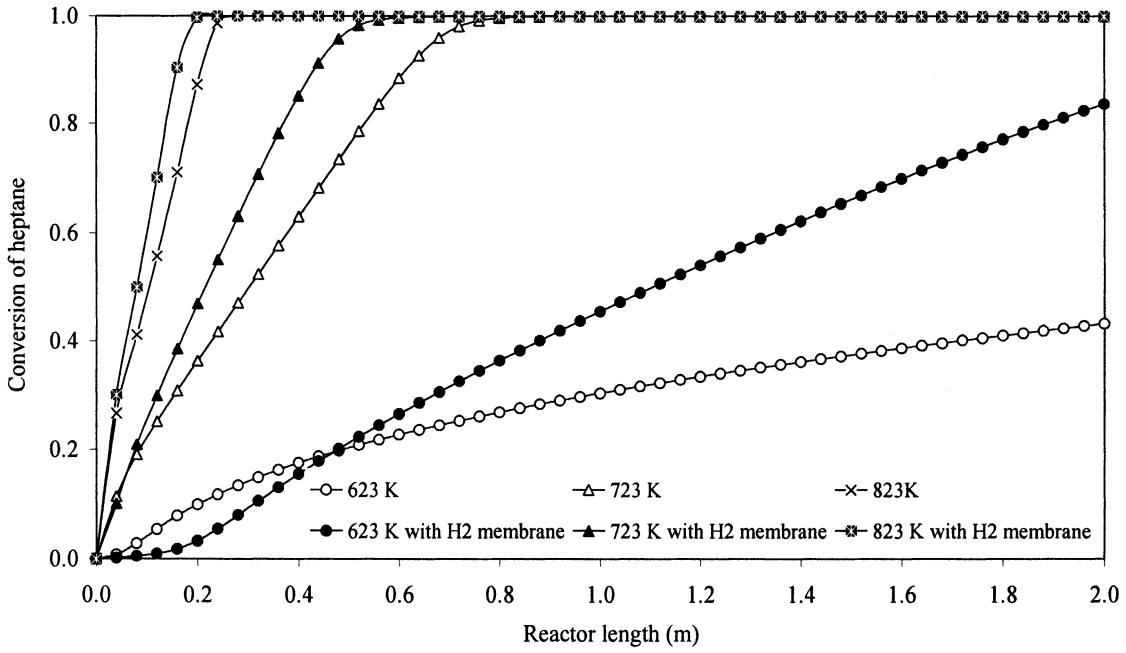

Figure 3. Effect of reaction temperature on the conversion of heptane under isothermal simulation.

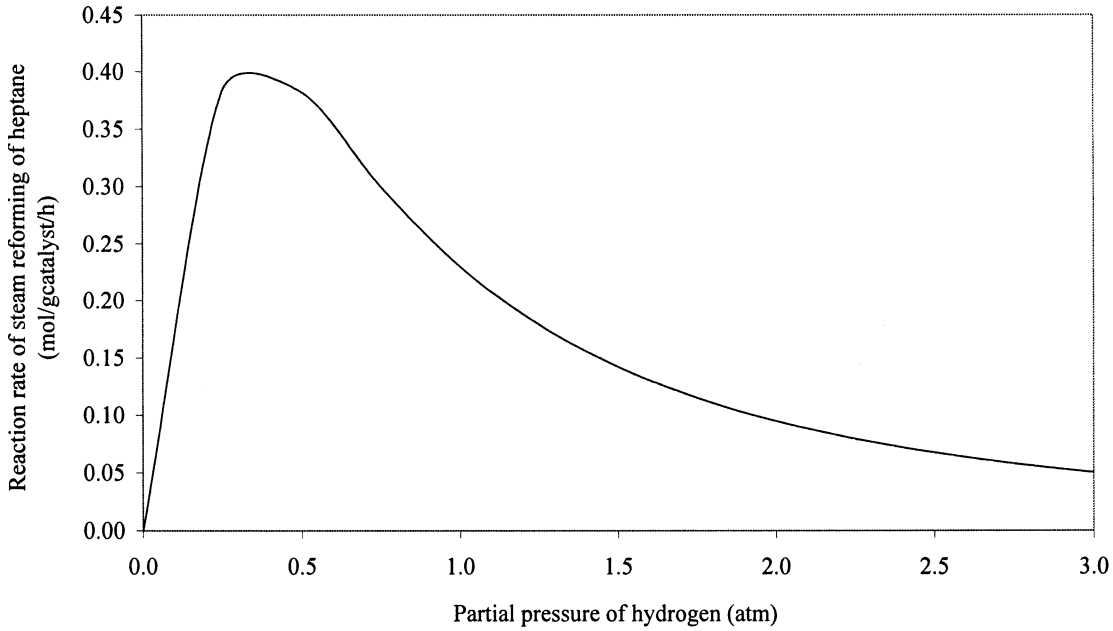

Figure 4. Reaction rate of steam reforming of heptane vs. the partial pressure of hydrogen.

the temperature increases for both cases without and with hydrogen membranes. With hydrogen membranes the conversion of heptane is greater than that without hydrogen membranes, making the reactor length for full conversion of heptane shorter. For example, at 723 K the reactor length for a full conversion of heptane is about 0.7 m without hydrogen membranes and about 0.5 m with hydrogen membranes, respectively. This phenomenon can be explained with the help of Figure 4, which is plotted according to the kinetic Eq. 4 for heptane steam reforming at the base set of reaction conditions (Table 1). It is found that the rate of heptane steam reforming is nonmonotonic with respect to the partial pressure of hydrogen. The rate increases as the partial pressure of hydrogen increases from 0 to 0.25 atm and then the rate decreases for the partial pressure of hydrogen above 0.25 atm. For most simulation cases the partial pressure of hydrogen is greater than 0.25 atm, therefore, the removal of product hydrogen by hydrogen permselective membranes, which decreases the partial pressure of hydrogen, will cause an increase in the rate for heptane steam reforming. As a result the conversion of heptane for the reformer with hydrogen membranes is higher than that without hydrogen membranes.

Figures 5 and 6 show the effects of reaction temperature on the yields of methane and hydrogen for the cases without and with only 10 hydrogen membranes. Obviously the steam reforming system approaches equilibrium quickly after the full conversion of heptane for the cases without hydrogen membranes, because the yields of methane and hydrogen are constant along the length after the full conversion of heptane. For example, at 723 K without hydrogen membranes the reactor length for the full conversion of heptane is about 0.7 m (Figure 3) and the reactor lengths for reaching the constant yields of methane and hydrogen are about 0.8 m and 1.0 m, respectively. Without hydrogen membranes, the methane and hydrogen yields increase quickly as the temperature increases due to the fast methanation and steam reforming of heptane. After the full conversion of heptane the yield of methane increases to a maximum and then keeps constant along the reactor length, while the yield of hydrogen decreases to a minimum and then keeps constant. The reason is that after the full conversion of heptane, the main sources for hydrogen production by heptane stops, while the methanation continues to consume hydrogen until the equilibrium state is reached, making the yield of methane higher (Figure 5) and the yield of hydrogen lower (Figure 6). At the low temperature 623 K, heptane is not fully converted; thus both the yields of methane and hydrogen increase along the reactor length. Figure 5 shows that the yield of methane is very low at 623 K, indicating that the methanation reaction is very slow at this temperature. With hydrogen membranes the yield of hydrogen is much higher than in the cases without hydrogen membranes due to the fact that the removal of hydrogen breaks the equilibrium state among the reversible reactions, specifically suppressing the extent of the methanation (as a result the yield of methane is much lower). Figure 6 also shows that the yield of hydrogen is nonmonotonic with respect to the reaction temperature. That is, the yields of hydrogen for both cases without and with hydrogen membranes are the lowest at 723 K for the three investigated temperatures. This is mainly due to the fact that the higher extent of methanation reaction at 723 K compared with that at both the lower temperature of 623 K and the higher temperature of 823 K. Specifically, at 623 K the methanation reaction is not so significant and, thus, makes the yield of methane negligible. While as the temperature increases, the methanation reaction becomes more and more significant, making the yield of methane higher at 723 K for both cases without and with hydrogen membranes. However, when the temperature increases to 823 K, the reverse of methanation (steam reforming of methane) increases, and the methanation is suppressed, especially in the presence of hydrogen membranes. As a result the yield of hydrogen at 723 K is the lowest and the yield of methane is the highest for both cases without and with hydrogen membranes. It is clear that steam reforming of

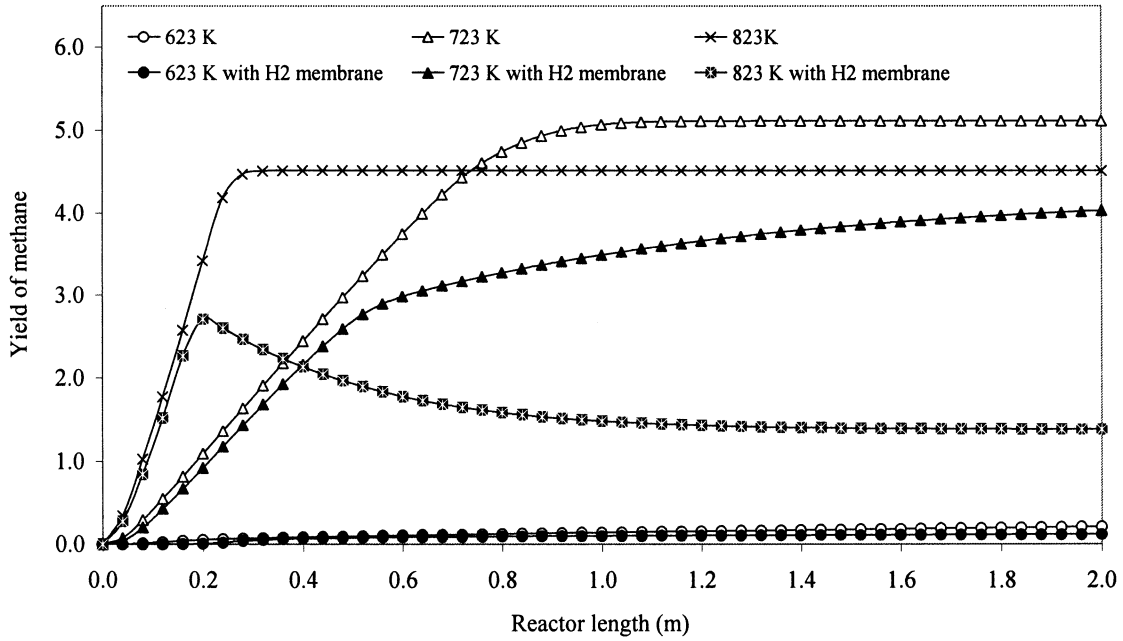

Figure 5. Effect of temperature on the yield of methane under isothermal simulation.

methane becomes more and more important for temperatures ≥ 823 K.

Table 2 compares the novel CFFBMR performance with the fixed-bed reformers (Rostrup-Nielsen, 1977; Phillips et al., 1970; Tottrup, 1982). Because there are few operating data published in the literature regarding steam reforming of heptane, the comparison becomes somewhat difficult. Thus, in this article the simulation conditions for the comparison are chosen almost the same as for the fixed-bed reformer operations. From Table 2 it is clear that the CFFBMR is much more efficient with regard to hydrogen yield and productivity.

Isothermal operations: effect of steam-to-carbon ratio without/with hydrogen selective membranes

Only the effect of the steam-to-heptane feed ratio is investigated in this section. The cases without/with 10 hydrogen membrane tubes are investigated under isothermal simula-

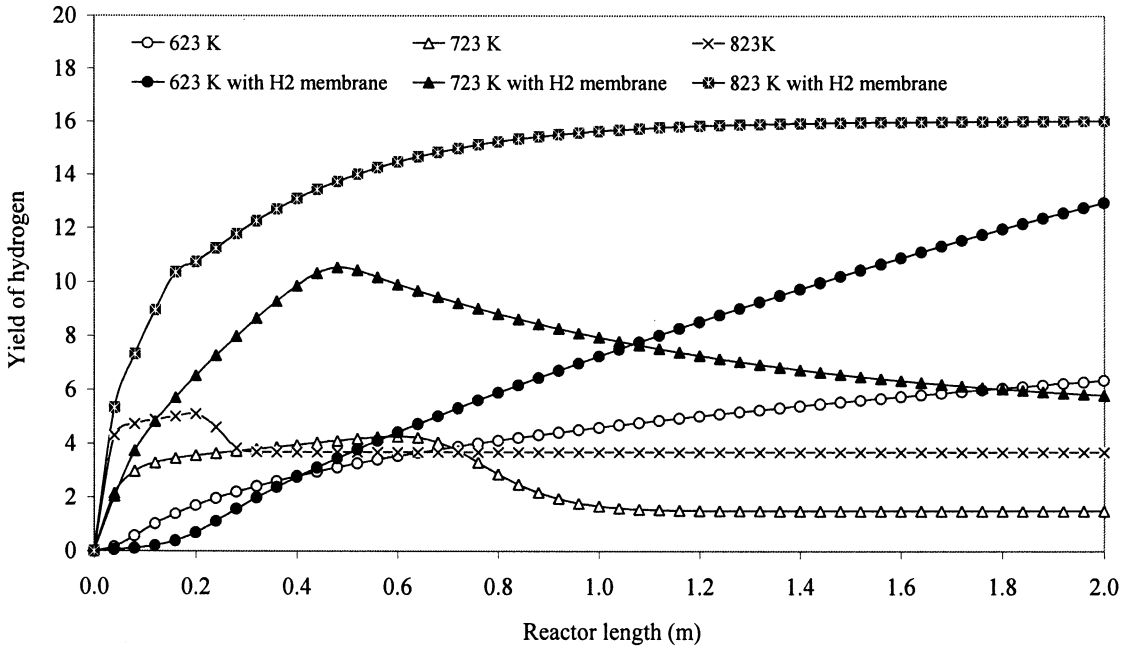

Figure 6. Effect of temperature on the yield of hydrogen under isothermal simulation.

Table 2. Performance Comparison Between the CFFBMR and the Fixed-Bed Reformers

	Fixed-Bed Reformer	CFFBMR	
Catalyst particle size (mm)	11*	0.186	
Effectiveness factor	<0.01	~1.0	
Gas velocity (m/s)	~1 m/s*	1 ~ 3 m/s	
Thermodynamic equilibrium	Limited	"Broken"	
Possibility of catalyst regeneration	No	Yes	
Huge furnace	Necessary	Unnecessary	
Volume of reformer	Large	Small	
Length of tube (m)	~ 10 m*	2	
Reaction temperature (K)	723.15**	723.15	823.15
Reaction pressure (atm)	14.7**	14.7	10
Heptane feed rate (mol/h)	NA	640	640
Steam-to-carbon feed ratio (mol/mol)	1.43**	1.43	2
Exit heptane conversion	1.0**	1.0	1.0
Exit steam conversion	0.44**	0.6106	0.7674
Hydrogen yield (mol/mol heptane fed)	2.0**	6.2669	16.023
Methane yield (mol/mol heptane fed)	5.2**	3.9194	1.3851
Yield of carbon monoxide (mol/mol heptane fed)	0.06**	0.0556	0.43795
Yield of carbon dioxide (mol/mol heptane fed)	1.8**	3.025	5.177
Membrane diameter (mm)	—	4.89	4.89
Hydrogen productivity (moles of hydrogen per hour per m^3 of reactor)	21,911†	267,089	662,875

*Data based on Rostrup-Nielsen (1977).
**Data based on Phillips et al. (1970).
†Data calculated based on Tottrup (1982).

tion. The emphasis is on the effect of the steam-to-carbon ratio on the reformer performance while neglecting the carbon formation, as explained earlier. Figure 7 shows the effect of the steam-to-carbon ratio on the yield of hydrogen at 723 K. The higher the steam-to-carbon ratio, the higher the yield of hydrogen. However, there is a maximum yield of hydrogen developed along the reactor length for both cases without and with hydrogen membranes. This is due to the full conversion of heptane at that position. In the reforming system when heptane is fully converted into carbon monoxide and hydrogen, the production of hydrogen by heptane stops. While the methanation continues to consume some hydrogen, making the hydrogen yield decrease. As a result a maximum hydrogen yield develops along the reforming bed. However, for the case without hydrogen membranes an equilibrium state develops quickly between the methanation, steam reforming of methane, and water gas shift reactions, making the hydrogen yield decrease toward a constant value. When the hydrogen product is removed by using hydrogen-selective membranes, this kind of equilibrium barrier is "broken," shifting the reactions (methanation or steam reforming of methane and water gas shift) toward higher hydrogen production. As a result the

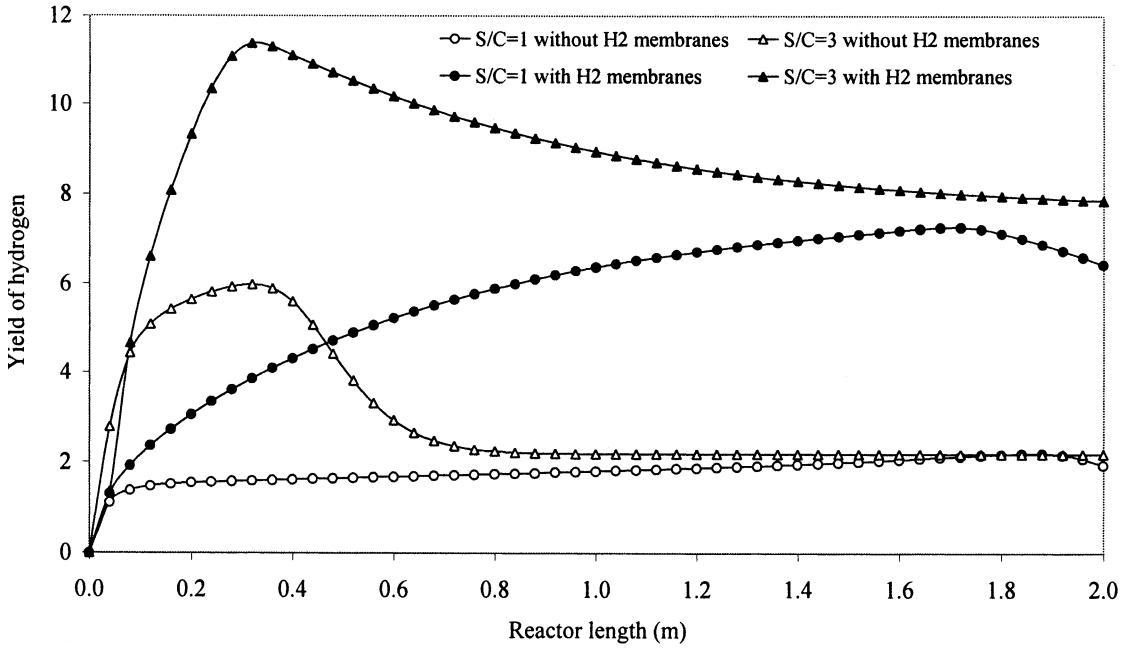

Figure 7. Effect of steam-to-carbon ratio on the yield of hydrogen.

yield of hydrogen is higher than the case without hydrogen membranes. Figure 7 shows that with hydrogen-selective membranes the reformer can produce higher hydrogen yield at a low steam-to-carbon ratio. For example, at a steam-to-carbon ratio of 1, the yield of hydrogen is 6.37 at 723 K for the case with hydrogen-selective membranes, while for the case without hydrogen membranes the yield of hydrogen is only 2 even at a higher steam-to-carbon ratio of 3.

Isothermal operations: effect of reaction pressure without/with hydrogen selective membranes

The effect of the reaction pressure on the yield of hydrogen is investigated at 723 K in this section without and with only 10 hydrogen membranes. Figure 8 shows the cases with operating pressures of 5, 10, and 20 atm that are simulated under isothermal conditions. As discussed earlier, there are maximum yields of hydrogen, which develops along the reactor length due to the full conversion of heptane at that position. Without hydrogen membranes, the hydrogen yield decreases as the operating pressure increases. After heptane is fully converted in the reformer, an equilibrium state is established in the bed, making the hydrogen yield constant along the rest of the length. The hydrogen yield is higher at a lower reaction pressure because of the increase in the number of moles accompanying the steam reforming process. For example, at 5 atm the hydrogen yield is 2.11 moles hydrogen per mole heptane fed, while the hydrogen yield is 1.50 at 10 atm. However, with hydrogen selective membranes, the yield of hydrogen is higher than that case without hydrogen membranes. For example, with hydrogen membranes the hydrogen yield is 3.85 at 5 atm and 5.80 at 10 atm, respectively. Again, the removal of hydrogen enhances the hydrogen production and suppresses the methanation in the reformer. Generally, the yield of hydrogen increases as the operating pressure increases when hydrogen-selective membranes are used. Therefore, using the hydrogen selective membranes the novel CFFBMR has the potential to produce a high yield of hydrogen at high operating pressures.

Nonisothermal operations: effect of heating policy without/with hydrogen-selective membranes

The four different heating policies shown in Figure 9 are utilized to study the nonisothermal CFFBMR performance for the cases without and with only 10 hydrogen membranes at a feed temperature of 723 K. The total heat supplies to the reformer are the same for the three nonadiabatic heating policies. With hydrogen-selective membranes the removal of hydrogen increases the yield of hydrogen for all the cases. The simulation results are summarized in Table 3. The hydrogen yield in Table 3 show the significance of the heating policies by this order: Decreasing heating policy > Uniform heating policy > Increasing heating policy > Adiabatic (no heat supply). As shown earlier, steam reforming of heptane occurs quite fast near the entrance of the reformer and the reaction length for full conversion of heptane is usually short; thus, under nonisothermal operation the heat supply rate required near the entrance of the reformer is quite a bit larger than at the other parts of the reformer. Otherwise the reforming rate will be very slow. Decreasing heating policy causes the largest heat flux near the entrance, making the temperature drop the least and keeping the system in the best state for endothermic steam reforming. As a result, the yield of hydrogen is the highest for the case with a decreasing heating policy among these four heating policies. From this simulation, it is clear that the most important heating part for steam reforming of heptane is near the entrance of the reformer.

Nonisothermal operations: effect of oxygen introduction as a feed without hydrogen- or oxygen-selective membranes

In this section oxygen is fed directly into the adiabatic reformer at a feed temperature of 773 K for oxidative reform-

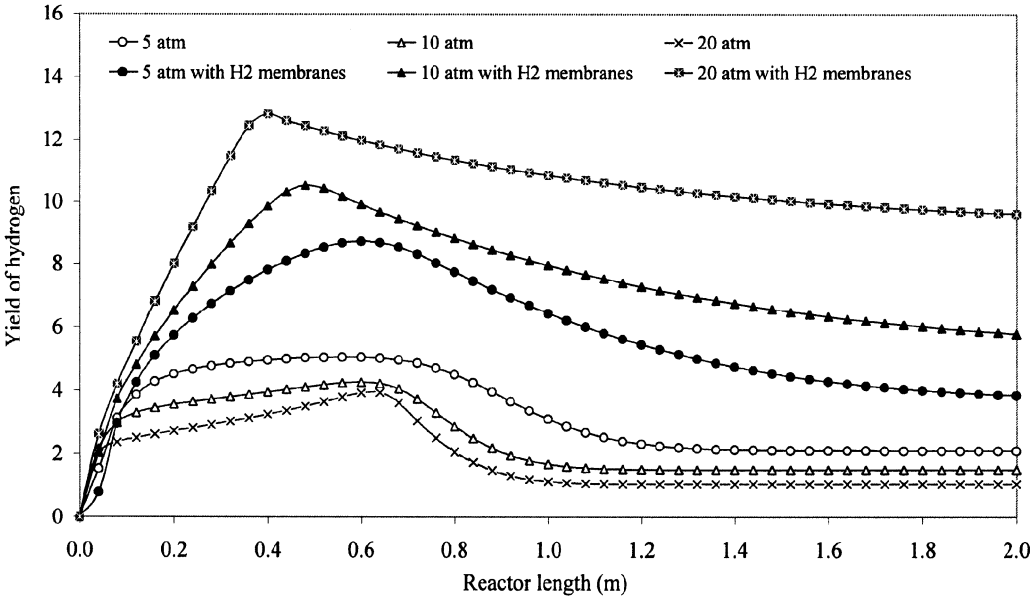

Figure 8. Effect of reaction pressure on the yield of hydrogen.

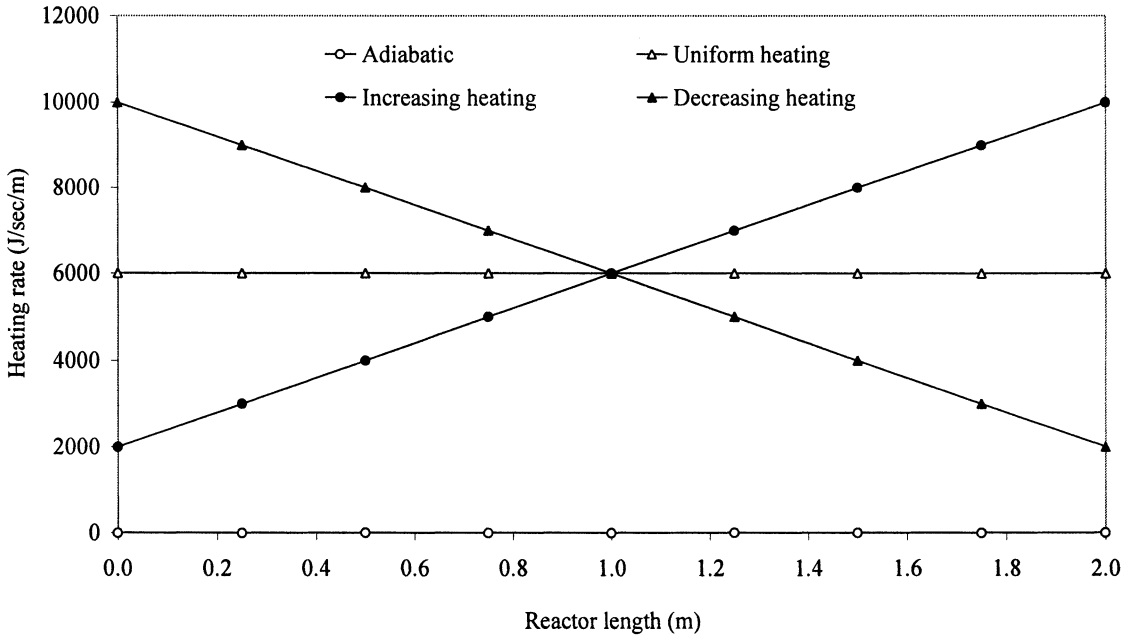

Figure 9. Four different heating policies for nonisothermal simulation.

ing of hydrocarbons without any hydrogen or oxygen membranes. The effects of oxygen direct feed on reformer performance are shown in Figures 10 (reactor temperature profile) and 11 (yield of hydrogen), respectively. The oxygen-to-heptane feed ratios of 0, 0.05, and 0.1 are used for this investigation and the heptane feed rate is 0.64 kmol/h.

It is found that the feed oxygen is fully consumed via the oxidative reforming of heptane and methane (byproduct) in the first half of the reformer. The exothermic oxidative reforming reactions release the heat of reaction to compensate for the endothermic nonoxidative steam reforming of heptane and methane. As a result the temperature profile along the reactor length is modified and increases with the increase of oxygen feed rate (Figure 11), making the reforming bed more efficient for steam reforming of hydrocarbons. At low oxygen-to-heptane feed ratios, the conversion of heptane is low, for example, at a oxygen-to-heptane feed ratio of 0.05, the exit conversion of heptane at 773 K is 0.61. After the full conversion of oxygen in the first half bed, there is no other heat supply for the adiabatic steam reforming. On the other hand, the endothermic steam reforming of heptane continues slowly due to the low temperature, as a result making the reactor temperature decrease slowly in the rest of the reformer. However, if the oxygen-to-heptane feed ratio is as high as 0.1 mol/mol, the exit conversion of heptane is 1 at the reactor length of 1.2 m. Since at 773 K the steam reforming of methane is not significant, as discussed earlier, after the full conversion of heptane the reforming system quickly establishes an equilibrium state in the reformer, making the profiles of the reactor temperature (Figure 10) and the yield of hydrogen (Figure 11) flat along the rest of the reactor length. The steep temperature drop near the entrance of the reformer is due to the steam reforming of heptane and its high endothermicity. The general increases in the conversion of heptane and the yield of hydrogen as the oxygen feed rate increases are evident. For example, without oxygen feed the hydrogen yield at a adiabatic operation is 4.74, while at oxygen to heptane feed ratio of 0.05 mol/mol, the hydrogen yield increases to 5.4. However, the hydrogen yield decreases at a high feed ratio of oxygen to heptane; for example, for the case of 0.1 mol/mol the hydrogen yield is 2.98. Similarly, as discussed earlier, this exception is due to the full conversion of heptane and the establishment of the equilibrium state in the bed. After the full conversion of heptane, the methanation reaction continues to consume some hydrogen until the equilibrium state is established, making the hydrogen yield decrease at that position. The equilibrium barrier can be "broken" by using the hydrogen-selective membranes, as demonstrated earlier. The combination of the endothermic steam reforming and exothermic oxidative reforming provides the possibility for adiabatic autothermal operations (Figure 10), which supports the viewpoint that autothermal conditions could be reached and maintained by oxygen addition in steam reformers (Roy et al., 1999).

Table 3. Hydrogen Yield at Different Heating Policies Under Nonisothermal Simulation

Heating Policy	Without H_2 Membranes	With H_2 Membranes	Improvement %
Adiabatic	3.5964	3.8962	8.34
Uniform	4.1158	4.4878	9.04
Increasing	4.0079	4.3836	9.38
Decreasing	4.2307	4.5980	8.68

Nonisothermal operations: effect of oxygen introduction using oxygen selective membranes

An alternate approach to introduce oxygen into the reformer is through oxygen-selective membranes, which allows the distribution of the supply of oxygen along the reformer

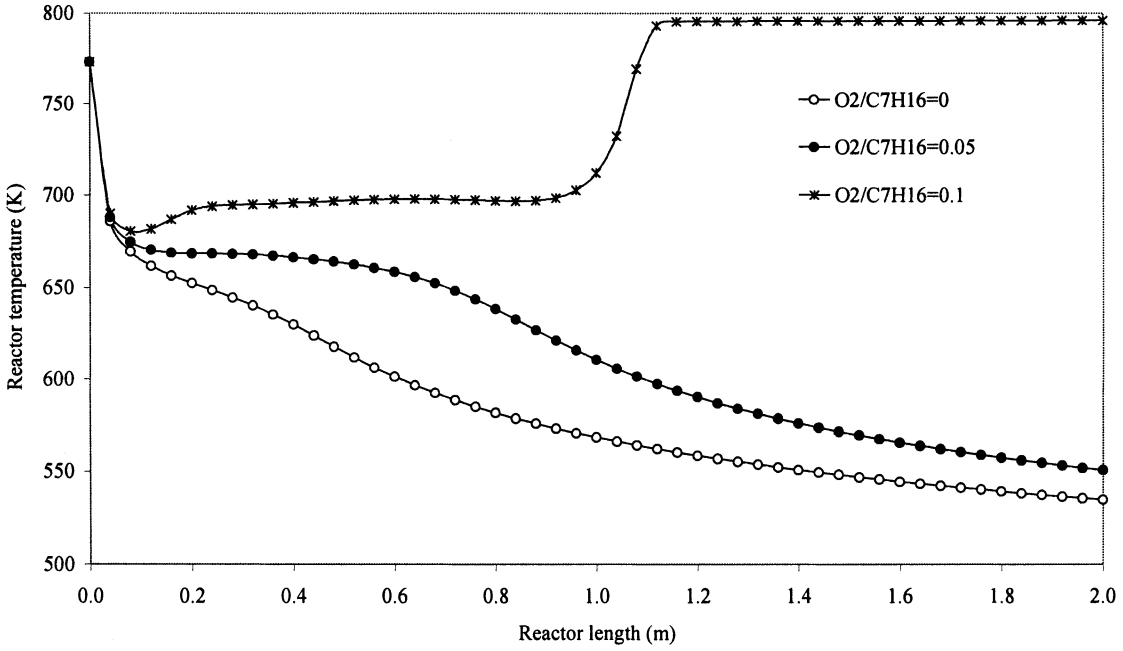

Figure 10. Effect of oxygen direct feed on the reactor temperature profile at adiabatic simulation.

height (or length) so as to allow the distribution of the exothermic oxidative reforming heat. Figures 12 and 13 show the effects of oxygen introduction by oxygen-selective membranes on the profiles of the reactor temperature and the yield of hydrogen, respectively. The oxygen permeation rate is temperature dependent, and the permeation rate increases as the temperature increases for dense perovskite oxygen membranes. The feed temperature is chosen to be 823 K in this section. Four numbers of oxygen-selective membranes are used: 0, 30, 60, and 90. According to the diameters of the reformer and oxygen membranes, the percentages of the reactor cross-sectional area occupied by oxygen membranes for the four cases are 0, 7.5%, 15%, and 22.5%, respectively. The fast steam reforming of heptane and its high endothermicity cause the reformer temperature to drop steeply near the entrance of the reformer, to about 125 K (Figure 12). As the reformer temperature decreases, the steam reforming rate decreases and the demand of heat supply for steam reform-

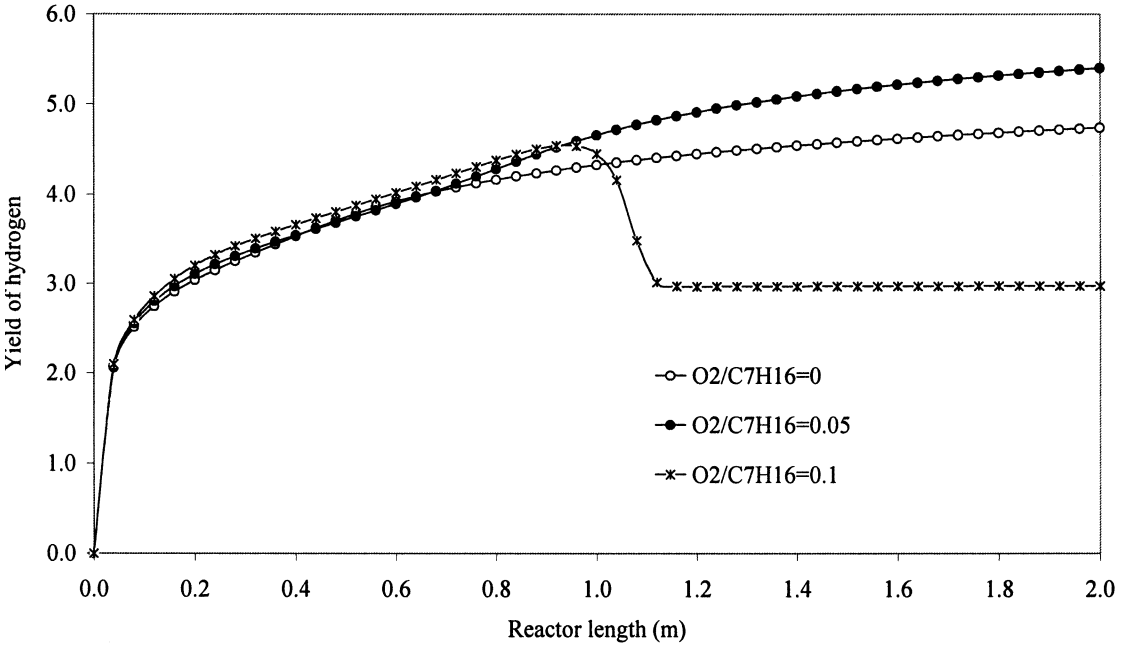

Figure 11. Effect of oxygen direct feed on the yield of hydrogen at adiabatic simulation.

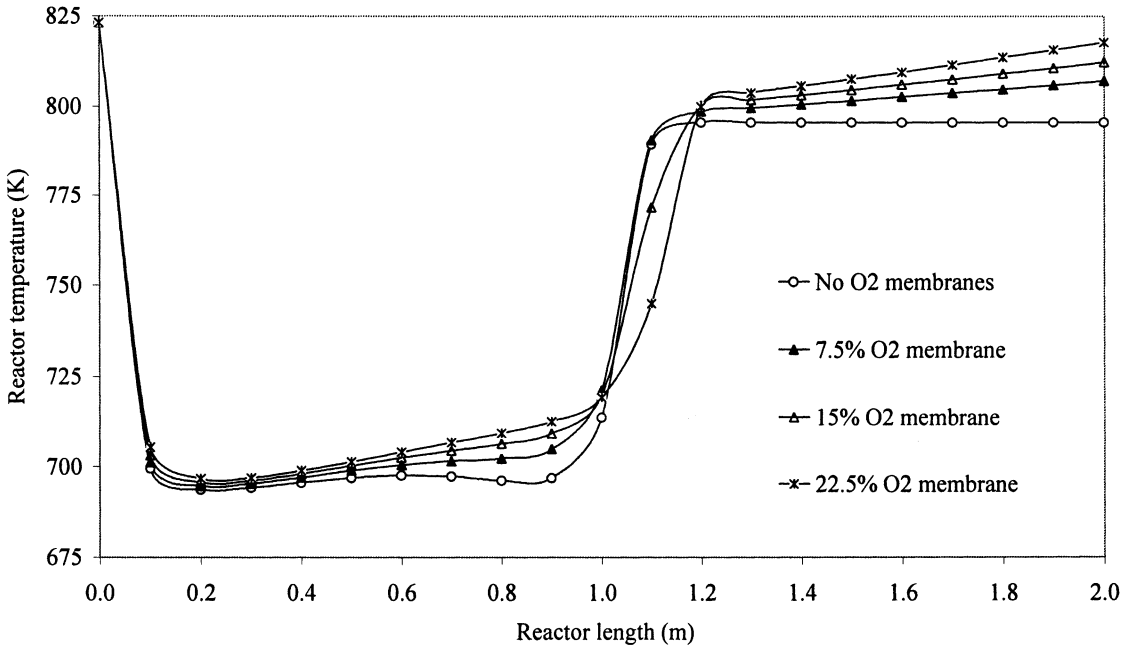

Figure 12. Effect of oxygen introduction by oxygen membranes on the reactor temperature.

ing decreases, too. At the same time, the oxidative reforming of heptane and methane product along the reformer height (length) supplies some of the heat needed for the endothermic steam reforming. As a result, the reformer temperature stops to decrease near a reformer height of 0.2 m, and then increases slowly until the full conversion of heptane is achieved near a reformer height of 1 m. After the full conversion of heptane, the process is dominated by the fast methanation, causing the hydrogen yield to decrease (Figure 13) and the temperature to increase (Figure 12) in the high reformer range of 1 m−1.2 m. Because oxygen permeates into the reformer continuously through oxygen-selective membranes for oxidative reforming of methane, which supplies the heat of reaction continuously after the full conversion of heptane, the reactor temperature increases along the rest of the reformer height, as shown in Figure 12. As a result of this continuous temperature increase, the hydrogen yield also increases continuously (Figure 13). The hydrogen yield in-

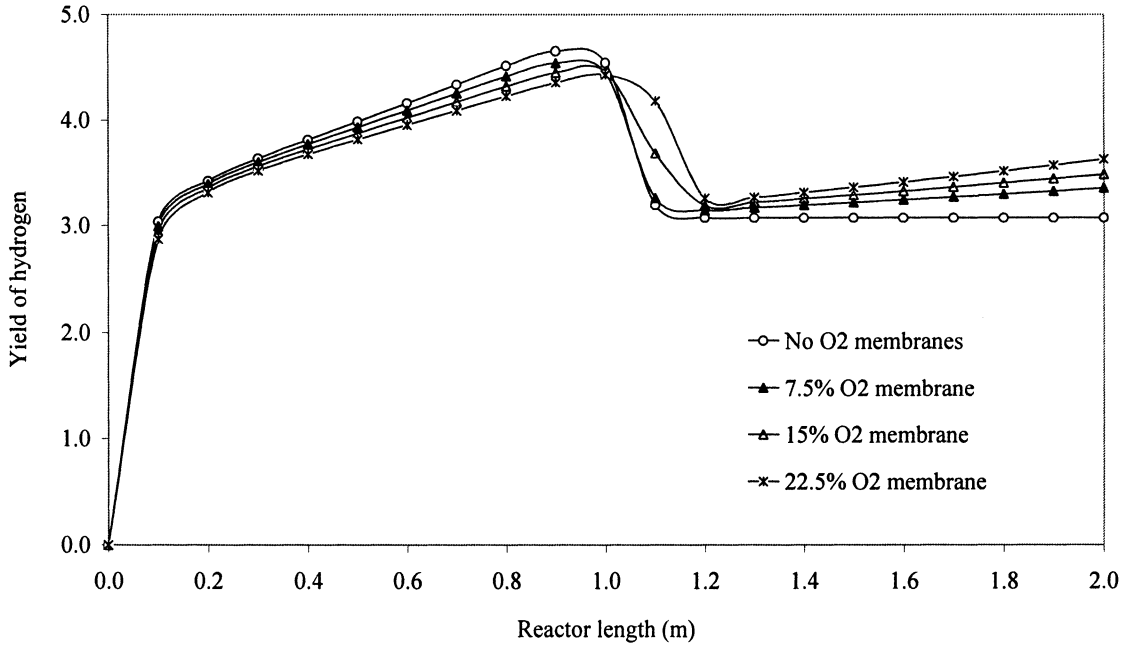

Figure 13. Effect of oxygen introduction by oxygen membranes on the yield of hydrogen.

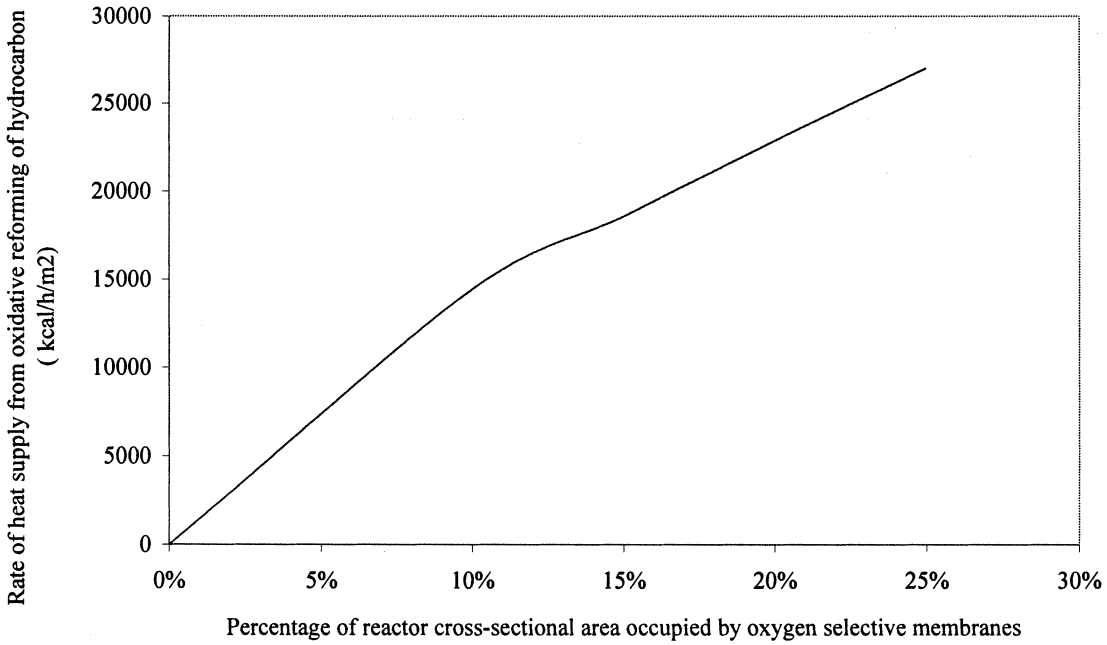

Figure 14. Rate of heat supply from oxidative reforming of hydrocarbons as a function of reactor cross-sectional area occupied by oxygen selective membranes at the feed temperature of 823 K.

creases as the number of oxygen-selective membranes increases for the four investigated adiabatic simulations. As shown in Figure 13, the hydrogen yields are 3.08, 3.36, 3.49, and 3.63, respectively. The heat released from the oxidative reforming is used fully in the reformer for endothermic steam reforming without any heat loss. Therefore, the use of oxygen-selective membranes has an energy-saving advantage over other external heating procedures. The reformer temperature profile in Figure 12 indicates that there is a large heat-supply demand near the entrance of the reformer. And it also shows that the exit reformer temperatures are close to the feed temperatures (near isothermal operation). Thus, the novel CFFBMR reformer can also be operated autothermally by using oxygen-selective membranes.

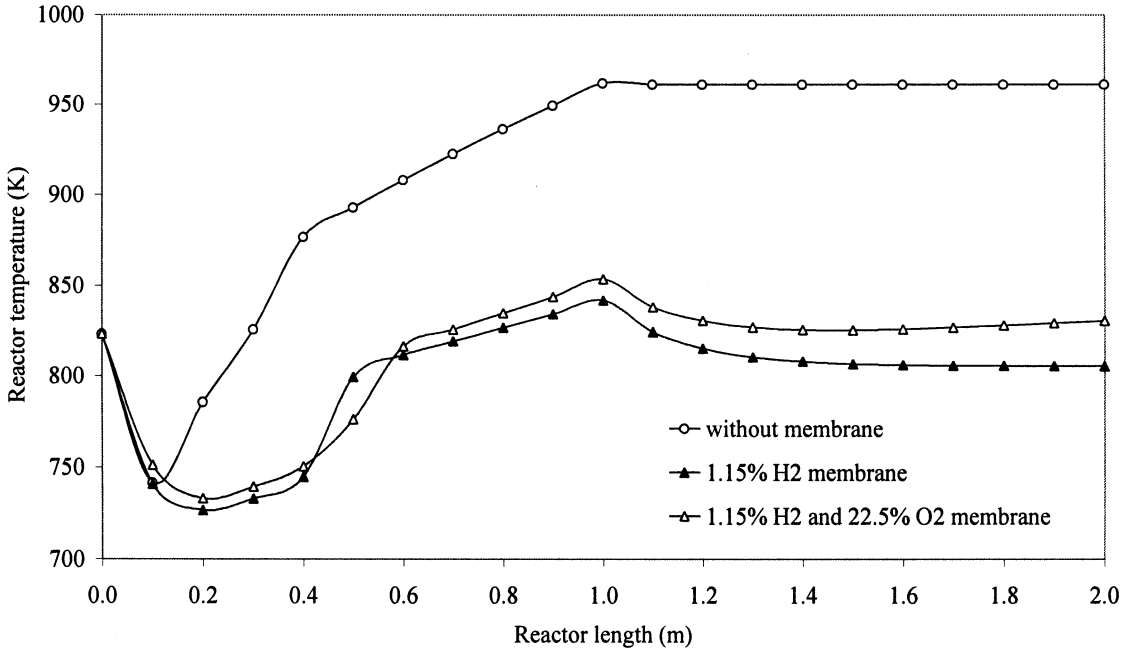

Figure 15. Reactor temperature profile by using hydrogen and oxygen membranes together with partial heating at the first half of the reformer under nonisothermal simulation.

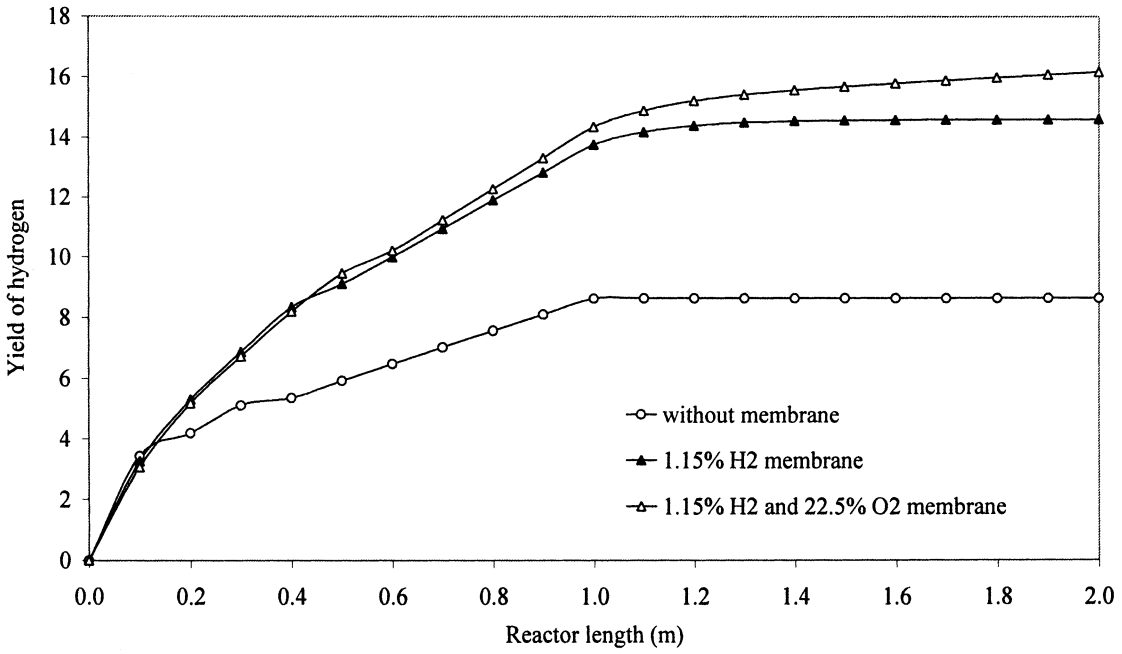

Figure 16. Yield of hydrogen by using hydrogen- and oxygen-selective membranes together with partial heating in the first half of the reformer under nonisothermal simulation.

In order to show the energy-saving advantage achieved by using oxygen membranes, Figure 14 shows the heat-supply rate from the oxidative reforming of hydrocarbons as a function of the reactor cross-sectional area occupied by oxygen membranes at a feed temperature of 823 K. For the case with a 22.5% cross-sectional area occupied by oxygen membranes, the heat-supply rate from oxidative reforming is about 25,000 kcal/h/m^2. Rostrup-Nielsen (1977) reported that the average external heating rate by a top- or side-fired furnace for steam reforming of naphtha is about 73,000 kcal/h/m^2 in an industrial fixed-bed reformer. Taking the heating efficiency of the industrial furnace and the heat transfer resistance between the furnace and the inside of the reformer tubes into consideration, the rates of heat supply for both cases are comparable. Thus, obviously the novel CFFBMR configuration has a very strong energy-saving potential.

Nonisothermal operations: effect of the combined use of hydrogen and oxygen membranes with partial heating

As just demonstrated, oxidative reforming of hydrocarbons can supply some of the heat needed for the endothermic steam reforming of heptane and methane product in the reformer with 100% heat efficiency. However, steep temperature drops near the entrance of the reformer occur in the adiabatic cases. The low reactor temperature, in turn, results in slow oxygen permeation flux in the oxygen membranes, and, thus, make the reforming rate slow. In order to improve the process further, the reformer performance is investigated under the combined use of hydrogen membrane tubes and oxygen membranes with partial heating of the reformer at a feed temperature of 823 K. Partial heating in this section means that the reformer is heated first at half the reformer height with a uniform heating rate of 90,000 J/h/m or 70 kcal/h/m^2. Figures 15 and 16 show the profiles of the reactor temperature and the yield of hydrogen for the following three cases with partial heating: (1) without any hydrogen or oxygen membranes; (2) with a 1.15% cross-sectional area occupied by hydrogen membranes (six hydrogen membrane tubes) only; and (3) with a 1.15% cross-sectional area occupied by hydrogen membranes together with a 22.5% occupation by oxygen membranes (90 oxygen membrane tubes). It's clearly shown that the problem of a large temperature drop near the entrance can be improved by a low heating rate in the first half of the reformer height, together with the combined use of the hydrogen- and oxygen-selective membranes. Figure 15 shows that without any membranes the reformer temperature increases to 960 K after the full conversion of heptane and the yield of hydrogen is 8.64. While when hydrogen membranes are used the reformer temperature is controlled to a very stable level and the hydrogen yield increases to 14.60. Furthermore the combined use of hydrogen and oxygen membranes improves this reformer temperature profile (Figure 15) so it is better for steam reforming of heptane with a higher yield of hydrogen of 16.18 (Figure 16). Figure 16 shows the general trend that by using hydrogen membranes the hydrogen yield is enhanced (14.60) and that by using both hydrogen and oxygen membranes, the yield of hydrogen is enhanced to a much higher value of 16.18. Thus, a combination of these two selective membranes provides a potential for the very efficient production of hydrogen by the steam reforming of heptane.

Optimization of Operating Parameters

The performance of the novel CFFBMR can be improved by using hydrogen- and oxygen-selective membranes, as well as the direct feed of oxygen. Different heating policies supply

different heat flux near the entrance of the reformer, thus improving the reactor temperature profile. Parameter optimization of the novel CFFBMR configuration is necessary for the efficient production of hydrogen. A large number of parameters could affect the reformer performance. For simplicity, only a small number of carefully determined parameters is used as the variables. The optimization objective, variables, and constraints are defined as follows:

Objective: $(Y_{H_2})_{max}$, Maximum yield of hydrogen

Variables:

N_{H_2} = number of hydrogen membrane tubes
N_{O_2} = number of oxygen membrane tubes
$F_{O_2,0}$ = oxygen direct-feed rate
S/C = steam-to-carbon (of heptane) feed ratio
Q = heating rate

From the previous investigation the most important heating part is near the entrance of the CFFBMR. In this optimization section, for maximum energy saving and the simplicity of optimization, only a uniform heating policy is applied on the first half of the CFFBMR.

Constraints:

(1) The percentage of the reactor cross-sectional area occupied by hydrogen and oxygen membranes should be below 50%. For the diameters of the reformer tube, hydrogen, and oxygen membranes as listed in Table 1, this constraint provides the following equation

$$\begin{cases} N_{H_2} + N_{O_2} \le 200 \\ N_{H_2} \ge 0 \\ N_{O_2} \ge 0 \end{cases} \tag{25}$$

(2) To avoid hot spots or "run away" in the CFFBMR, and also to avoid extinction of the reforming and loss of the catalyst activity, the reactor temperature should be well controlled for safe operation. Thus, the range of the operating temperature for steam reforming of heptane in CFFBMR is chosen as

$$500 \le T \le 1{,}250 \text{ K} \tag{26}$$

(3) In order to save on operating costs, the ratio of steam to carbon is limited below 4 mol/mol in this part of the investigation. According to the stoichiometry for steam reforming of heptane, the minimum ratio of steam to carbon is 1; thus

$$1 \le S/C \le 4 \tag{27}$$

In short the parameter optimization process can be summarized as the following function

Objective:

$$(Y_{H_2})_{max} = f(N_{H_2}, N_{O_2}, F_{O_2,0}, S/C, Q) \tag{28}$$

Subject to:

$$\begin{cases} N_{H_2} + N_{O_2} \le 200 \\ N_{H_2} \ge 0 \\ N_{O_2} \ge 0 \\ 500 \le T \le 1{,}250 \text{ K} \\ 1 \le S/C \le 4 \\ F_{O_2,0} \ge 0 \end{cases} \tag{29}$$

Table 4. Parameter Optimization Result for Steam-Reforming of Heptane in CFFBMR

Optimal Variables and Yield of Hydrogen	
Number of hydrogen membranes (N_{H_2})	140.367
Number of oxygen membranes (N_{O_2})	23.063
Oxygen feed rate ($F_{O_2,0}$ in kmol/h)	3.698
Steam-to-carbon feed ratio (S/C)	4.002
Heating rate (J/h/m)	27,216
Maximum yield of hydrogen (mol/mol heptane fed)	11.771

Note: Reaction conditions for optimization are listed in Table 1, except the variables.

Using the flexible tolerance optimization method (FTOM) (Himmelblau, 1972), the parameters for the CFFBMR are optimized according to the objective function and constraints just defined. Table 4 shows the parameter optimization result for the base set of reaction conditions, as listed in Table 1, except the optimization variables. The reported yield of hydrogen by steam reforming of heptane at 723 K is about 2 in fixed-bed reformers due to the thermodynamic equilibrium limitation (Phillips et al., 1970), while the yield of hydrogen resulting from this optimization reaches about 11.8. The improvement is about 490% in the yield of hydrogen. Obviously the CFFBMR has the advantage to produce hydrogen efficiently with much higher yield and with minimum energy consumption.

Conclusions

Because steam reforming of hydrocarbon is an endothermic reaction, high temperatures are required for industrial operations. However, equilibrium states develop quickly among the reversible methanation, steam reforming of methane, and water–gas shift reactions. The equilibrium states limit the production of hydrogen, making the yield of hydrogen much lower and the yield of methane much higher in the reformer. The continuous removal of hydrogen from the reformer using hydrogen-selective membranes breaks the equilibrium barriers and improves the performance of the reformer as well as suppressing the methane yield and increasing the hydrogen yield. The novel CFFBMR has the advantages of producing pure hydrogen with a high yield even at low temperatures, low steam-to-carbon feed ratios, and at high reaction pressures. The process simulations show that the steam reforming of heptane in the CFFBMR is very fast, especially at high temperatures above 723 K, because the diffusion limitations are eliminated by using fine catalyst particles in the novel reformer, making the novel reformer highly efficient for hydrogen production. Because of the large endothermicity of the fast steam reforming of heptane, the demand for heat supply near the entrance of the CFFBMR reformer is quite large. With the introduction of oxygen into the steam reformer, the oxidative reforming of heptane and

methane product releases some of the heat needed for the endothermic steam reforming and also produces some hydrogen. Oxygen can be fed directly or through oxygen-selective membranes. The distribution of oxygen along the reactor length through oxygen membranes improves the reactor temperature profile in the bed. As a result, it improves the performance of the novel CFFBMR reformer. The combination of the endothermic steam reforming and exothermic oxidative reforming of hydrocarbons by using both hydrogen- and oxygen-selective membranes not only enhances the yield of hydrogen, but also saves energy. Based on the investigation of the effects of the operating parameter on the novel CFFBMR performance, the parameter optimization is conducted using the flexible tolerance optimization method. The optimization result shows that the hydrogen yield by steam reforming of heptane can be significantly increased with minimum energy consumption.

Literature Cited

Adris, A. M., S. S. E. H. Elnashaie, and R. Hughes, "A Fluidized Bed Membrane Reactor for the Steam Reforming of Methane," *Can. J. Chem. Eng.*, **69**(10), 1061 (1991).

Adris, A., J. Grace, C. Lim, and S. S. E. H. Elnashaie, "Fluidized Bed Reaction System for Steam/Hydrocarbon Gas Reforming to Produce Hydrogen," U.S. Patent No. 5,326,550 (June, 1994a).

Adris, A. M., C. J. Lim, and J. R. Grace, "The Fluidized Bed Membrane Reactor (FBMR) System: A Pilot Scale Experimental Study," *Chem. Eng. Sci.*, **49**, 5833 (1994b).

Adris, A. M., C. J. Lim, and J. R. Grace, "The Fluidized-Bed Membrane Reactor for Steam Methane Reforming: Model Verification and Parametric Study," *Chem. Eng. Sci.*, **52**, 1609 (1997).

Alhabdan, F. M., M. A. Abashar, and S. S. E. H. Elnashaie, "A Flexible Software Package for Industrial Steam Reformers and Methanators Based on Rigorous Heterogeneous Models," *Math. Comput. Model.*, **16**, 77 (1992).

Armor, J. N., "The Multiple Roles for Catalysis in the Production of H_2," *Appl. Catal. A: Gen.*, **176**, 159 (1999).

Ashcroft, A. T., A. K. Cheetham, J. S. Foord, M. L. H. Green, C. P. J. Grey, A. Murrell, and P. D. F. Vernon, "Selective Oxidation of Methane to Synthesis Gas Using Transient Metal Catalysis," *Nature*, **344**, 319 (1990).

Avc, A. K., Z. I. Onsan, and D. L. Trimm, "On-Board Fuel Conversion for Hydrogen Fuel Cells: Comparison of Different Fuels by Computer Simulations," *Appl. Catal. A: Gen.*, **216**, 243 (2001).

Barbieri, G., and F. P. Di Maio, "Simulation of Methane Steam Reforming Process in a Catalytic Pd-Membrane Reactor," *Ind. Eng. Chem. Res.*, **36**, 2121 (1997).

Blank, R. F., T. S. Wittrig, and D. A. Peterson, "Bidirection Adiabatic Synthesis Gas Generator," *Chem. Eng. Sci.*, **45**, 2407 (1990).

Chen, Z., P. Prasad, and S. S. E. H. Elnashaie, "The Coupling of Catalytic Steam Reforming and Oxidative Reforming of Methane to Produce Pure Hydrogen in a Novel Circulating Fast Fluidized Bed Membrane Reformer," *Fuel Chem. Div. Preprints*, ACS Meeting, Orlando, FL (2002).

Christensen, T. S., "Adiabatic Prereforming of Hydrocarbons—An Important Step in Syngas Production," *Appl. Catal. A: Gen.*, **138**, 285 (1996).

Ding, Y., and E. Alpay, "Adsorption-Enhanced Steam-Methane Reforming," *Chem. Eng. Sci.*, **55**, 3929 (2000).

Elnashaie, S. S. E. H., M. E. Abashar, and A. S. Al-Ubaid, "Simulation and Optimization of an Industrial Ammonia Reactor," *Ind. Eng. Chem. Res.*, **27**, 2015 (1988).

Elnashaie, S. S. E. H., and A. Adris, "Fluidized Bed Steam Reformer for Methane," *Proc. Int. Fluidization Conf.*, Banff, Canada, May (1989).

Elnashaie, S. S. E. H., and S. S. Elshishini, *Modelling, Simulation and Optimization of Industrial Fixed-Bed Catalytic Reactors*, Gordon & Breach, London (1993).

Froment, G. F., "Production of Synthesis Gas by Steam- and CO_2-Reforming of Natural Gas," *J. Mol. Catal. A: Chem.*, **163**, 147 (2000).

Grace, J. R., "Contacting Modes and Behavior Classification of Gas-Solid and Other Two-Phase Suspension," *Can. J. Chem. Eng.*, **64**, 353 (1986).

Groote, A. M. D., and G. F. Froment, "Simulation of the Catalytic Partial Oxidation of Methane to Synthesis Gas," *Appl. Catal. A: Gen.*, **138**, 245 (1996).

Haider, A., and O. Levenspiel, "Drag Coefficient and Terminal Velocity of Spherical and Nonspherical Particles," *Powder Technol.*, **58**, 63 (1989).

Himmelblau, D. M., *Applied Nonlinear Programming*, McGraw-Hill, New York, p. 341 (1972).

Hou, K., M. Fowles, and R. Hughes, "The Effect of Hydrogen Removal During Methane Steam Reforming in Membrane Reactors in the Presence of Hydrogen Sulphide," *Catal. Today*, **56**, 13 (2000).

Jin, W., X. Gu, S. Li, P. Huang, N. Xu, and J. Shi, "Experimental and Simulation Study on a Catalyst Packed Tubular Dense Membrane Reactor for Partial Oxidation of Methane to Syngas," *Chem. Eng. Sci.*, **55**, 2617 (2000).

Kunii, D., and O. Levenspiel, *Fluidization Engineering*, 2nd ed., Butterworth-Heineman, Stoneham, MA (1991).

Kunii, D., and O. Levenspiel, "Circulating Fluidized-Bed Reactors," *Chem. Eng. Sci.*, **52**(15), 2471 (1997).

Ostrowski, T., A. Giroir-Fendler, C. Mirodatos, and L. Mleczko, "Comparative Study of the Catalytic Partial Oxidation of Methane to Synthesis Gas in Fixed-Bed and Fluidized-Bed Membrane Reactors, Part I: A Modeling Approach," *Catal. Today*, **40**, 181 (1998).

Phillips, T. R., J. Mulhall, and G. F. Turner, "The Kinetics and Mechanism of the Reaction Between Steam and Hydrocarbons over Nickel Catalysts in the Temperature Range 350−500°C, Part I," *J. Catal.*, **15**, 233 (1969).

Phillips, T. R., J. Mulhall, and G. F. Turner, "The Kinetics and Mechanism of the Reaction Between Steam and Hydrocarbons over Nickel Catalysts in the Temperature Range 350−500°C, Part II," *J. Catal.*, **17**, 28 (1970).

Rostrup-Nielsen, J. R., "Activity of Nickel Catalysts for Steam Reforming of Hydrocarbons," *J. Catal.*, **31**, 173 (1973).

Rostrup-Nielsen, J., "Hydrogen via Steam Reforming of Naphtha," *Chem. Eng. Prog.*, **9**, 87 (1977).

Roy, S., B. B. Pruden, A. M. Adris, C. J. Lim, and J. R. Grace, "Fluidized Bed Steam Methane Reforming with Oxygen Input," *Chem. Eng. Sci.*, **54**, 2095 (1999).

Shu, J., B. P. A. Grandjean, and S. Kaliaguine, "Methane Steam Reforming in Asymmetric Pd- and Pd-Ag/porous SS Membrane Reactor," *Appl. Catal.*, **119**, 305 (1994).

Siminski, V. J., F. J. Wright, R. B. Edelman, C. Economos, and O. F. Fortune, "Research on Methods of Improving the Combustion Characteristics of Liquid Hydrocarbon Fuels," *AFAPL TR 72-74*, Vols. I and II, Air Force Aeropropulsion Laboratory, Wright Patterson Air Force Base, OH (1972).

Tottrup, P. B., "Evaluation of Intrinsic Steam Reforming Kinetic Parameters from Rate Measurments on Full Particle Size," *Appl. Catal.*, **4**, 377 (1982).

Tsai, C.-Y., A. G. Dixon, W. R. Moser, and Y. H. Ma, "Dense Perovskite Membrane Reactors for Partial Oxidation of Membrane to Syngas," *AIChE J.*, **43**(11A), 2741 (1997).

Twigg, M. V., *Catalyst Handbook*, 2nd ed., Wolfe, London, England, p. 225 (1989).

Wurzel, T., and L. Mleczko, "Engineering Model of Catalytic Partial Oxidation of Methane to Synthesis Gas in a Fluidized-Bed Reactor," *Chem. Eng. J.*, **69**, 127 (1989).

Xu, J., and G. F. Froment, "Methane Steam Reforming, Methanation and Water-Gas Shift: I. Intrinsic Kinetics," *AIChE J.*, **35**(1), 88 (1989).

Manuscript received May 21, 2002, revision received Oct. 9, 2002, and final revision received Dec. 18, 2002.